

Cerebral functional abnormalities in patients with nasopharyngeal carcinoma after radiotherapy: an observational magnetic resonance resting-state study

Wen-Ting Ren¹, Ye-Xiong Li¹, Kai Wang¹, Li Gao¹, Jun-Lin Yi¹, Xiao-Dong Huang¹, Jing-Wei Luo¹, Run-Ye Wu¹, Yong Yang¹, Jian-Yang Wang¹, Wen-Qing Wang¹, Jing-Bo Wang¹, Feng Ye², Han Ouyang², Jian-Rong Dai¹

¹Department of Radiation Oncology, National Cancer Center/National Clinical Research Center for Cancer/Cancer Hospital, Chinese Academy of Medical Sciences and Peking Union Medical College, Beijing 100021, China;

²Department of Diagnostic Radiology, National Cancer Center/National Clinical Research Center for Cancer/Cancer Hospital, Chinese Academy of Medical Sciences and Peking Union Medical College, Beijing 100021, China.

Abstract

Background: Nasopharyngeal carcinoma (NPC) is sensitive to radiotherapy (RT). However, neurocognitive complications such as memory loss and learning and attention deficits emerge in the survivors of NPC who received RT. It remains unclear how radiation affects patient brain function. This pilot study aimed at finding cerebral functional alterations in NPC patients who have received RT.

Methods: From September 2014 to December 2016, 42 individuals, including 22 NPC patients and 20 normal volunteer controls in National Cancer Center/National Clinical Research Center for Cancer/Cancer Hospital, Chinese Academy of Medical Sciences, and Peking Union Medical College, were recruited in this study. All patients received resting-state functional magnetic resonance imaging scans and neurocognitive tests 1 day before the initiation of RT (baseline) and 1 day after the completion of RT; the 20 normal controls were also subjected to the same scans and tests. The amplitude of the low-frequency fluctuations (ALFF) in blood oxygen level-dependent signals and functional connectivity (FC) were used to characterize cerebral functional changes. Independent *t* test, paired *t* test, and analysis of variances were used to obtain statistical significance across groups.

Results: After RT, NPC patients showed significantly decreased ALFF values in the calcarine sulcus, lingual gyrus, cuneus, and superior occipital gyrus and showed significantly reduced FC mainly in the default mode network ($P < 0.05$, corrected by AlphaSim). Relative to the controls, ALFF was decreased in the lingual gyrus, calcarine sulcus, cingulate cortex, medial prefrontal gyrus ($P < 0.05$, corrected by AlphaSim), and FC reduction was found in multiple cerebellar–cerebral regions, including the cerebellum, parahippocampus, hippocampus, fusiform gyrus, inferior frontal gyrus, inferior occipital gyrus, precuneus, and cingulate cortex ($P < 0.001$, corrected by AlphaSim).

Conclusions: Cerebral functional alterations occur immediately after RT. This study may provide an explanation for the cognitive deficits in the morphologically normal-appearing brains of NPC patients after RT and may contribute to the understanding of the complex mechanism of RT.

Keywords: Radiotherapy; Nasopharyngeal carcinoma; MRI; Functional

Introduction

Nasopharyngeal carcinoma (NPC) is an endemic disease and radiotherapy (RT) is the mainstay method for treatment.^[1] Despite a high 5-year overall survival rate, the survivors of NPC always develop neurocognitive complications such as memory loss, cognitive impairment, and neuropsychological dysfunctions.^[2-4] These neurocognitive complications can be long lasting and can greatly affect the patients' living quality.^[5] With the development of RT technology, the radiation dose on brain tissue has

been greatly decreased, and the number of patients with brain tissue necrosis has been greatly reduced.^[6,7] However, neurocognitive complications can still be observed in surviving NPC patients without overt cerebral morphologic injury.^[8] In fact, based on previous experimental data in rodent models, a radiation dose lower than 10 Gy is sufficient to cause cognitive dysfunction, although it is far from the lethal dose limit.^[9,10] This reminds us that the radiation affecting brain tissue may involve both morphologic and functional aspects.

Access this article online

Quick Response Code:



Website:
www.cmj.org

DOI:
10.1097/CM9.0000000000000277

Correspondence to: Prof. Jian-Rong Dai, Department of Radiation Oncology, National Cancer Center/National Clinical Research Center for Cancer/Cancer Hospital, Chinese Academy of Medical Sciences and Peking Union Medical College, Beijing 100021, China
E-Mail: dai_jianrong@163.com

Copyright © 2019 The Chinese Medical Association, produced by Wolters Kluwer, Inc. under the CC-BY-NC-ND license. This is an open access article distributed under the terms of the Creative Commons Attribution-Non Commercial-No Derivatives License 4.0 (CCBY-NC-ND), where it is permissible to download and share the work provided it is properly cited. The work cannot be changed in any way or used commercially without permission from the journal.

Chinese Medical Journal 2019;132(13)

Received: 28-12-2018 Edited by: Li-Min Chen

Previous researchers have proven that radiation can affect brain functions in neuronal dendritic complexity, synaptic protein levels, and neurotransmitter alterations using *ex vivo* animal slices.^[11,12] As *in vivo* study has shown that radiation is associated with functional brain alterations in patients with acute lymphoblastic leukemia after cranial RT,^[13] but until recently, little was known about the impact of radiation on the functional alterations in NPC patients after RT. Recently, a research team has suggested that radiation can induce functional connectivity (FC) alterations using two independent samples (one group comprised untreated NPC patients and the other comprised NPC patients 6 months after receiving RT), but it is still difficult to directly and objectively demonstrate the functional changes because it is hard to avoid various confounders from two different samples in these studies.^[14,15]

Resting-state functional magnetic resonance imaging (fMRI) has been reckoned as a powerful tool to investigate brain functional information under normal or pathological conditions and is easier to implement in clinical studies.^[16] The amplitude of low-frequency fluctuations (ALFF) (0.01–0.08 Hz) in the blood oxygenation level-dependent signal in resting-state fMRI data is thought to reflect spontaneous neural activity.^[17] Because the ALFF does not require a predefined region of interest and could be used for coordinate-based meta-analysis, it has been widely employed to study abnormal brain activities in many brain disorders.^[18,19] In addition to the ALFF, resting-state fMRI could also provide information about the FC of the whole brain, which is an analysis of the cross-correlations between spatially remote regions allowing the integrity of distributed brain networks to be examined.^[20]

In the present investigation, resting-state fMRI was used to reveal cerebral alterations in both neural activity and FC in NPC patients who have received RT, with the purpose of exploring whether RT could lead to brain function

alterations in the short-term, providing promising novel neuroimaging approaches to investigate radiation effects and trying to explain late radiation effects such as neurocognitive deficits in NPC patients without overt morphologic changes.

Methods

Ethical approval

The study was conducted in accordance with the *Declaration of Helsinki* and was approved by the local ethics committee of the National Cancer Center/Cancer Hospital, Chinese Academy of Medical Sciences, National GCP Center of Anticancer Drugs (NCC2014G-41). Informed written consent was obtained from all the participants prior to their enrollment in this study.

Participants

In this study, 42 right-handed individuals were recruited from our department from September 2014 to December 2016, including 22 newly diagnosed NPC patients and 20 healthy comparison controls. All the NPC patients had specific pathological examinations and were diagnosed by experienced radiologists (stages T2–T4). Healthy controls were recruited by poster advertisement with the age, gender, weight, handedness, and years of education matched to the NPC group [Table 1]. All controls were confirmed for the lifetime absence of psychiatric illnesses. Additionally, control participants were interviewed to ascertain that there was no history of psychiatric illness in first-degree relatives. The following exclusion criteria were applied to all the participants: distant metastasis, history of RT or chemotherapy, induction chemotherapy, organic brain disorder, drug or alcohol abuse, pregnancy or any physical illness, such as hepatitis, cardiovascular disease, and epilepsy or neurological disorders, as assessed by interview and review of medical records.

Table 1: Demographic information and neurocognitive tests scores for NPC patients and healthy controls.

Characteristic	NPC patients (n = 20)	Healthy controls (n = 17)	Statistics	P
Age (years)	46.30 ± 8.07	42.88 ± 8.31	1.27*	0.21
Education (years)	12.30 ± 4.54	14.00 ± 3.48	-1.26*	0.22
Weight (kg)	74.20 ± 8.59	70.82 ± 10.13	1.10*	0.28
Gender (M/F)	16/4	14/3	-	-
Handedness	Right-handed	Right-handed	-	-
Stage (UICC 2010)				
I/II	2	-	-	-
III/IV	18	-	-	-
With/without chemotherapy	12/8	-	-	-
MoCA (pre-RT/post-RT)	27.25 ± 1.68/27.00 ± 2.05	27.50 ± 1.82	-0.24 [†]	0.71
AVLT (pre-RT/post-RT)				
Immediate recall	9.97 ± 2.03/10.42 ± 2.35	11.10 ± 1.89	1.33 [†]	0.27
Delayed recall	10.30 ± 3.23/10.80 ± 3.25	11.41 ± 2.43	0.62 [†]	0.54
Delayed recognition	13.95 ± 1.32/13.55 ± 1.43	13.83 ± 1.29	0.46 [†]	0.63
SDS (pre-RT/post-RT)	31.00 ± 3.34/31.55 ± 3.82	29.71 ± 2.14	1.56 [†]	0.22
SAS (pre-RT/post-RT)	33.45 ± 2.70/33.10 ± 2.95	31.94 ± 2.05	1.63 [†]	0.21

Data are shown as n or mean ± standard deviation. * t value. [†] F value. -: not available; AVLT: Auditory verbal learning test; MoCA: Montreal Cognitive Assessment; NPC: Nasopharyngeal carcinoma; RT: Radiotherapy; SAS: Self-rating anxiety scale; SDS: Self-rating depression scale.

All NPC patients received resting-state fMRI scanning 1 day before the initiation of RT (baseline) and 1 day after the completion of RT treatment. The two scanning intervals were approximately 7 weeks. Controls were scanned only once to define the range of normal function because in an independent pilot study of 10 healthy participants scanned twice using the resting-state paradigm with a 7-week interval, we found no significant changes in the ALFF ($P > 0.05$). This observation is consistent with the previous studies, indicating a high level of consistency over time in resting-state ALFF measurements in healthy individuals.^[21] Brain magnetic resonance images (T1-weighted and T2-weighted images) were inspected by an experienced neuroradiologist, and no gross abnormalities were observed in any participant.

Neurocognitive tests, including the Montreal Cognitive Assessment (MoCA), self-rating depression scale, self-rating anxiety scale, and auditory verbal learning test (immediate recall, delayed recall, and delayed recognition), were administered to every NPC patients 1 day before the initiation of RT and 1 day after the completion of RT [Table 1]. One physician, who had been trained by an experienced clinical psychiatrist, obtained these neurocognitive tests results from all of the participants.

fMRI data acquisition

All participants were scanned on a 3T magnetic resonance scanner (Discovery MR750; General Electric Medical Systems, Milwaukee, WI, USA) and were required to close their eyes throughout the entire scanning time. High-resolution T1-weighted volumetric 3D images were obtained using a spoiled gradient recall sequence (repetition time [TR] = 8.5 ms, echo time [TE] = 3.2 ms, flip angle = 12°, slice thickness = 1 mm) with an eight-channel phased-array head coil. A field of view of 240 mm × 240 mm was used, with an acquisition matrix comprising 256 readings of 256 phase-encoding steps and an in-plane resolution approximately 1 mm × 1 mm. The values for the ALFF of the blood oxygenation level-dependent signal were obtained using a gradient-echo echo-planar imaging sequence (TR/TE = 2000/30 ms; flip angle = 90°). The slice thickness was 5 mm (no slice gap), with a matrix size of 64 mm × 64 mm and a field of view of 240 mm × 240 mm, resulting in a voxel size of 3.75 mm × 3.75 mm × 5 mm. Each brain volume comprised 30 axial slices, and each functional run contained 200 image volumes. Two patients and three controls with excessive head motion (translation of more than 1.5 mm or rotation of more than 1.5°) were excluded, resulting in samples of 20 patients and 17 controls in statistical analyses.

ALFF calculation

The ALFF was calculated using Data Processing Assistant for Resting-State fMRI (DPARSF, version 4.0, Beijing China), implemented with MATLAB toolbox (<http://www.rfmri.org>).^[22] Briefly, after converting DICOM files to NIFTI images, the first 10 time points were removed. Next, slice timing and head motion correction were performed. The data were then realigned and normalized using a standard echo-planar imaging

template and resampled to a 3 mm × 3 mm × 3 mm voxel size. After smoothing with a 6-mm Gaussian kernel, the time series were transformed to the frequency domain using fast Fourier transform, and the power spectrum was acquired. The averaged square root of the activity in this frequency band (0.01–0.08 Hz) was taken as the ALFF. For standardization purposes, ALFF maps of each voxel were divided by the global mean ALFF value to standardize the data across participants.

FC analysis

For the FC calculation, a seed voxel correlation approach was used.^[23] Based on the ALFF analysis results, the peak MNI coordinate with a spherical radius of 6 mm was defined as a seed. The detailed analyses were as follows. The resting-state fMRI Data Analysis Toolkit (REST, version 1.8, <http://www.restfmri.net>) was used for FC calculation.^[24] After bandpass filtering (0.01–0.08 Hz) and linear-trend removal, a reference time series for the seed was extracted. Correlation analysis was carried out between the seed and rest of the brain in a voxelwise manner. We removed components with high correlation to cerebrospinal fluid or white matter or with low correlation to gray matter, which are thought to be associated with artifacts such as cardiac-induced or respiratory-induced variations. The correlation coefficients in each voxel were transformed to z values using the Fisher r -to- z transformation to improve normality. Spatial smoothing was applied with an 8-mm³ full-width half-maximum Gaussian kernel. Next, the connectivity maps were obtained for statistical calculation.

Radiotherapy

All patients were treated with the intensity modulated radiation therapy technique randomly using the Varian-600CD (Varian Medical Systems, Palo Alto, CA, USA) or Helical TomoTherapy (Accuray Inc., Sunnyvale, CA, USA) linac with a prescribed dose of 70 to 80 Gy in 33 to 36 fractions. The treatment plans were designed on Pinnacle³ 9.0 treatment planning systems (Philips, Fitchburg, WI, USA) or TomoTherapy Planning System (Accuray Inc., Madison, WI, USA) using computed tomography datasets with a 3-mm slice thickness. The beam energy for all plans was 6 megavolt, and the ultimate goal of optimization for an individual patient plan was that the dose to organs at risk (OARs) can be kept as low as possible while maintaining optimal target coverage and dose uniformity to the target. Twelve of 20 patients received RT concurrent with chemotherapy, depending on their grade of disease.

Statistical analysis

The primary analyses involved a comparison of patients before and after RT in terms of regional cerebral ALFF values and FC by the seed voxel method. Paired t tests were used to calculate the significant differences, with a threshold $P < 0.05$. Secondary analyses separately compared the data before and after RT with the data from healthy participants. These analyses used independent t tests, and a significant statistical threshold was set at

$P < 0.05$ (for the comparison of ALFF values). For the comparison of FC, we chose $P < 0.001$ as the significant statistical threshold based on the present statistical results. All statistical analyses were performed using REST software, and all statistical threshold P value were corrected by multiple comparisons with the AlphaSim program, which is implemented in REST software based on the Monte Carlo simulation in AFNI software. Demographic information and neurocognitive test comparisons between patients before and after RT and with healthy controls were adopted using independent t test (two samples) and analysis of variance (three samples) in SPSS, version 22.0 (SPSS Inc., Chicago, IL, USA), with a threshold of $P < 0.05$.

Results

Demographic and neurocognitive tests

Table 1 summarizes and compares demographic information of the participants. There were no significant differences between the NPC patients and healthy controls in terms of age, education, weight, gender, and handedness. For neurocognitive tests, there were no significant changes

in patients before and after RT and healthy controls [Table 1], a finding that was not surprising given the short time interval.

Regional cerebral functions

After treatment, ALFF values in patients decreased in the bilateral calcarine sulcus and the lingual gyrus, cuneus, and superior occipital gyri [Table 2 and Figure 1]. Relative to the controls, patients showed no significant changes in ALFF values before RT. However, after RT, ALFF values significantly decreased in the lingual gyrus, calcarine sulcus, and medial prefrontal gyri and the cingulate cortex [Table 2 and Figure 2].

Neural network functions

FC analyses showed that after 7 weeks of RT, FC was significantly reduced between the seed and several cortical regions that were mainly involved in the default-mode network (DMN), including the precuneus, posterior cingulate cortex, medial prefrontal cortex, and some other regions such as the parahippocampus, cuneus, lingual

Table 2: Regions that showed significant changes in ALFF values and functional connectivity between the baseline and after RT in NPC patients and between NPC patients and controls.

Brain regions	Coordinates (x, y, z)	Cluster size	t	Side
ALFF				
Patients: week 7 of RT treatment: < baseline				
Calcarine sulcus (BA 18)	18, -69, 14	326	-2.90	R and L
Lingual gyrus (BA 19)	23, -53, -9	207	-4.46	R and L
Cuneus (BA 18)	17, -72, 20	207	-3.58	R and L
Superior occipital gyrus (BA 19)	24, -81, 42	44	-2.56	R and L
After RT treatment: patients < controls				
Lingual gyrus (BA 18)	6, -69, -6	198	-4.58	R and L
Calcarine sulcus (BA 17)	-12, -63, 9	189	-2.50	R and L
Medial prefrontal gyrus (BA 8)	3, 33, 60	228	-3.94	R and L
Cingulate cortex (BA 32)	6, 32, 24	86	-2.98	R and L
Functional connectivity				
Patients: week 7 of RT treatment: < baseline				
Precuneus (BA 23)	10, -65, 27	598	-4.05	R and L
Lingual gyrus (BA 37)	23, -50, -8	294	-4.26	R and L
Fusiform gyrus (BA 37)	21, -50, -11	263	-4.18	R and L
Cuneus (BA 23)	9, -67, 26	198	-4.10	R and L
Calcarine sulcus (BA 30)	-13, -49, 8	209	-3.12	R and L
Parahippocampus (BA 37)	18, -41, -3	70	-2.96	R and L
Cingulate cortex (BA 23, 32)	-8, -43, 33	320	-3.27	R and L
Medial prefrontal gyrus (BA 10)	-13, 51, 5	220	-2.89	R and L
Superior frontal gyrus (BA 10)	-14, 69, 17	102	-4.21	R and L
After RT treatment: patients < controls				
Cerebellum (BA 30, 37)	12, -66, -45	341	-5.34	R and L
Hippocampus (BA 27)	-19, -29, -6	18	-4.67	R and L
Parahippocampus (BA 35)	19, -15, -23	44	-5.51	R and L
Fusiform gyrus (BA 37)	27, -42, -15	44	-3.80	R and L
Inferior occipital gyrus (BA 19)	-39, -72, -6	20	-4.13	L
Inferior frontal gyrus (BA 45)	57, 39, 6	102	-5.57	R and L
Cingulate cortex (BA 23)	-8, -9, 35	20	-4.45	R and L
Precuneus (BA 7)	9, -42, 51	38	-4.32	R and L

ALFF: Amplitude of low-frequency fluctuations; BA: Brodmann area; L: Left; NPC: Nasopharyngeal carcinoma; R: Right; RT: Radiotherapy.

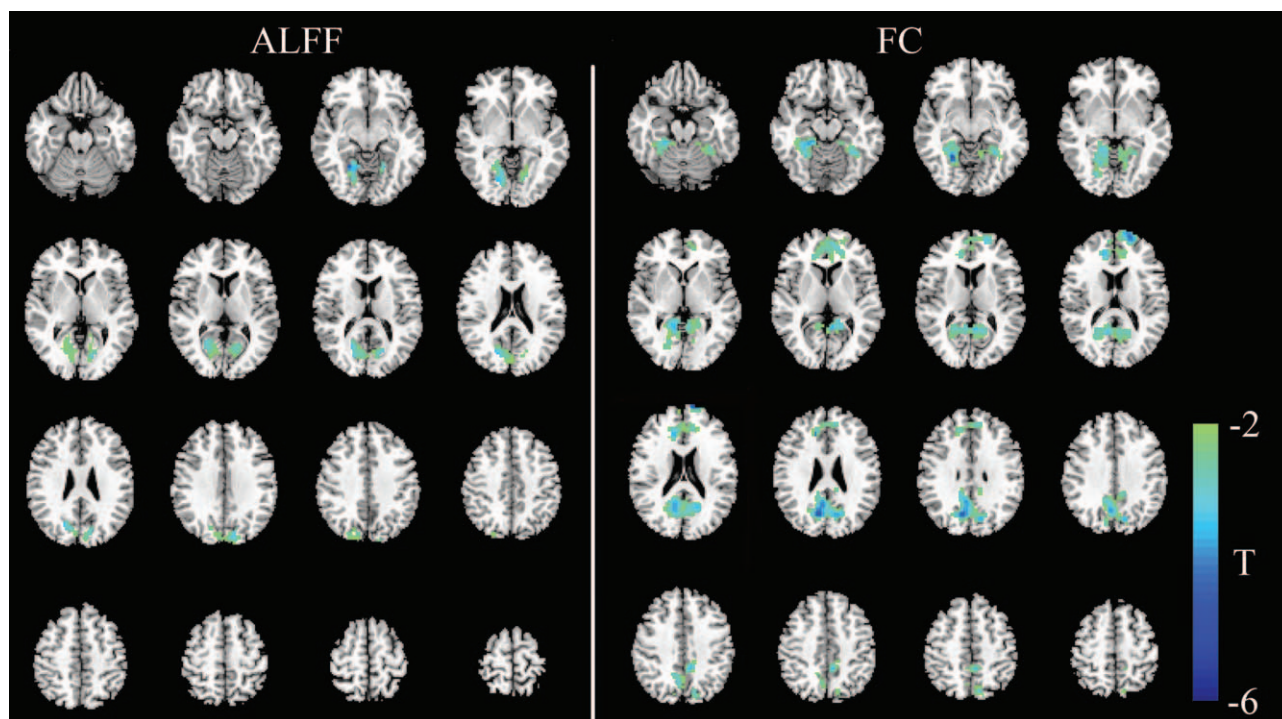


Figure 1: Significant differences in the cerebral functional alterations of NPC patients before and after RT. The left part shows regions with an abnormal ALFF, and the right part shows abnormal regions of functional connectivity. For NPC patients before and after RT, decreased ALFF values were mainly found in the bilateral cerebral regions, including the calcarine sulcus, lingual gyrus, cuneus, and superior occipital gyrus (left). Decreased FC values were mainly seen in the default mode network, including the precuneus, PCC, mPFC, parahippocampus, lingual gyrus, fusiform gyrus, calcarine sulcus, and cuneus (right) ($P < 0.05$, corrected for multiple comparisons with the AlphaSim program). ALFF: Amplitude of low-frequency fluctuation; FC: Functional connectivity; mPFC: Medial prefrontal cortex; NPC: Nasopharyngeal carcinoma; PCC: Posterior cingulate cortex; RT: Radiotherapy.

gyrus and fusiform gyri, and calcarine sulcus [Table 2 and Figure 1]. There was no significant difference in connectivity before RT. After RT, patients showed decreased connectivity in multiple cerebellar–cerebral regions, including the cerebellum, parahippocampal gyrus, hippocampus, fusiform gyrus, inferior frontal gyrus, inferior occipital gyrus, precuneus, and cingulate cortex, compared with controls [Table 2 and Figure 2].

OAR dose

The detailed dosimetric results of major OARs for all NPC patients are shown in Table 3. The dose–volume histogram for a representative patient is shown in Figure 3.

Discussion

Using the comparison data from NPC patients before and after RT, this study revealed cerebral functional deficits immediately after radiation treatment. After approximately 7 weeks of RT, NPC patients showed significantly decreased ALFF values relative to those during pretreatment in the bilateral calcarine sulcus, the lingual gyrus and superior occipital gyri, and the cuneus. For FC, significantly decreased correlations were mainly in the DMN, including the precuneus, posterior cingulate cortex and medial prefrontal cortex. Compared with the controls, there were no significant differences in ALFF values and FC before RT. However, patients after RT showed regional function changes and FC alterations in

several regions. These findings indicated that radioactive rays influenced human brain functions much earlier than morphologic changes. This may be the potential reason that cognitive impairments emerge in the normal-appearing brain of NPC patients after RT.

In the present study, we found that ALFF values decreased in the bilateral calcarine sulcus, lingual gyrus, cuneus, and superior occipital gyrus after RT. Generally, these regions have been regarded as visual centers, and previous functional MRI results have shown that dysfunction in these regions is related to visual problems.^[25,26] Regarding surviving NPC patients, numerous studies have suggested that many patients develop impairment of the optic path, such as visually evoked potential changes, radiation retinopathy, and dry eye syndrome, 1 to 22 years after RT.^[27] The functional alterations in the visual cortex in our study may be the early signs for these visual problems. In addition to the visual functions, recently, some studies have found that these occipital regions are related to cognitive deficits and working memory impairment in patients with diseases such as Alzheimer's disease^[28] and generalized anxiety disorder.^[29] These findings remind us that the late complications in cognitive deficits such as poor memory may also be related to these regions. Although the exact physiopathological mechanism of these regional functional changes is unclear, our findings provide new insights into the radiation-induced neural activity impairments and may show the most sensitive regions affected by RT. Further research is needed to clarify its cause and consequences.

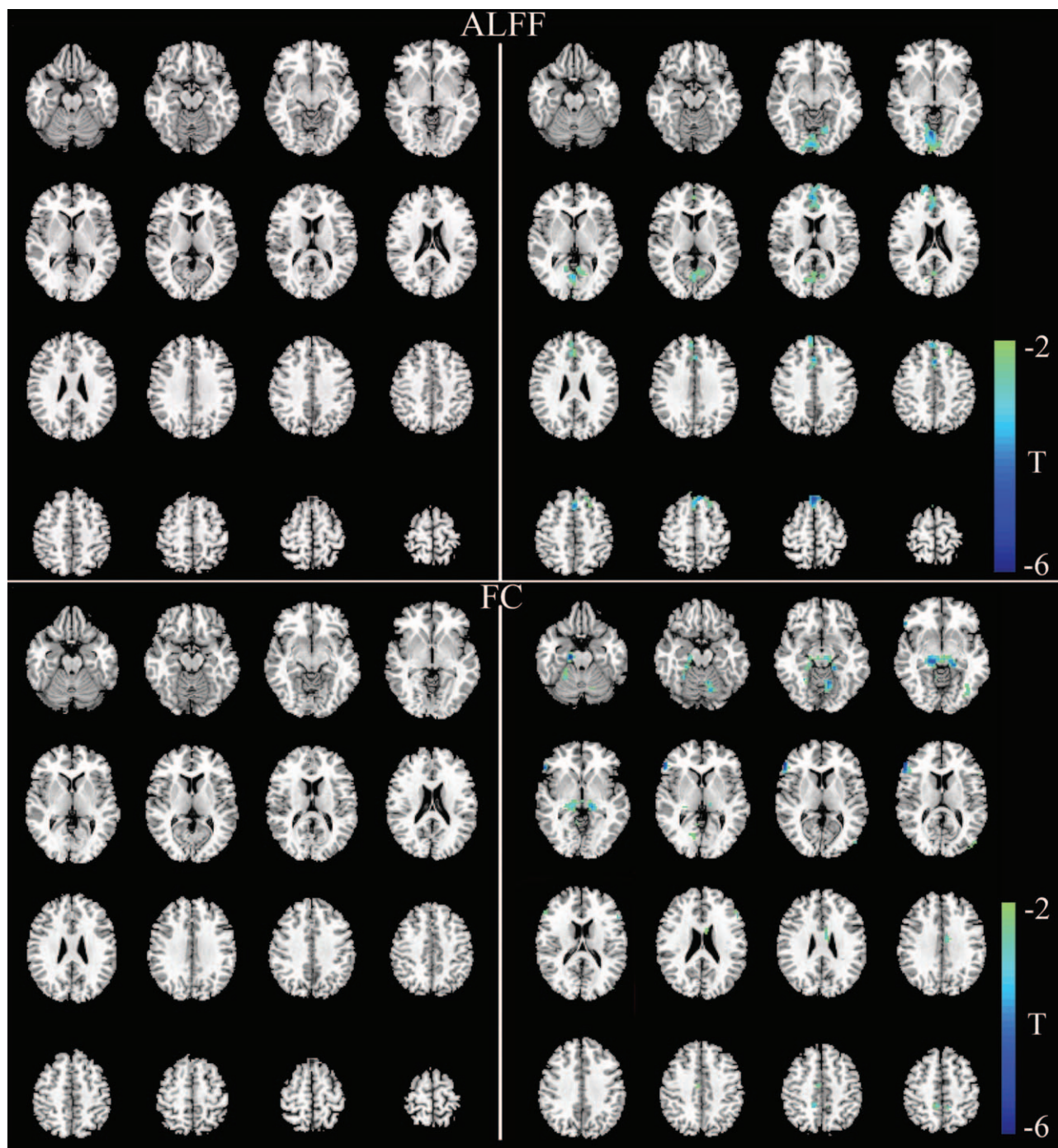


Figure 2: Significant differences in the ALFF values and functional network connectivity between NPC patients and healthy controls. The left part shows abnormal regions in NPC patients before RT compared with healthy controls, and the right part shows abnormal regions in NPC patients after RT compared with healthy controls. There are no significant changes in ALFF values and FC before RT (upper and lower left). After RT, decreased ALFF values were observed in the lingual gyrus, calcarine sulcus, medial prefrontal gyrus, and cingulate cortex (upper right) ($P < 0.05$, corrected for multiple comparisons with the AlphaSim program). Decreased FC values were observed in multiple cerebellar-cerebral regions, including the cerebellum, parahippocampus, hippocampus, fusiform gyrus, inferior frontal gyrus, inferior occipital gyrus, precuneus, and cingulate cortex (lower right) ($P < 0.001$, corrected for multiple comparisons with the AlphaSim program). ALFF: Amplitude of low-frequency fluctuation; FC: Functional connectivity; NPC: Nasopharyngeal carcinoma; RT: Radiotherapy.

Regarding the FC results, our study identified decreased FC mainly in the DMN in the survivors of NPC patients after RT. DMN is thought to represent self-projection, scene-construction, cognitive sciences and so on.^[30,31] Previous studies have suggested that the activity of DMN was decreased in normal aging persons with cognitive decline and Alzheimer's disease patients.^[32,33] These findings

demonstrated that DMN is associated with neurocognitive alterations. Recently, Ma *et al.*^[14,15] found that the abnormalities of DMN in the NPC patients after RT 6 to 87 months later. They selected 10 or 160 seed regions to detect alterations in FC, and significant correlations were observed between the functional connections and MoCA scores. In our study, we also found alterations in FC after

Table 3: Detailed dosimetric results of major OARs in NPC patients.

OARs	Dose (Gy, mean \pm SD)	OARs	Dose (Gy, mean \pm SD)
Brain stem		Spinal cord	
D _{mean}	26.30 \pm 3.82	D _{mean}	20.14 \pm 2.98
D _{max}	58.11 \pm 9.30	D _{max}	33.25 \pm 3.94
Left lens		Right lens	
D _{mean}	5.17 \pm 1.31	D _{mean}	5.19 \pm 1.19
D _{max}	7.49 \pm 1.80	D _{max}	7.33 \pm 1.76
Left optic nerve		Right optic nerve	
D _{mean}	43.69 \pm 14.61	D _{mean}	42.51 \pm 15.06
D _{max}	58.31 \pm 16.61	D _{max}	57.59 \pm 17.26
Optic chiasma		Pituitary	
D _{mean}	49.31 \pm 19.31	D _{mean}	59.86 \pm 15.00
D _{max}	60.18 \pm 17.87	D _{max}	68.78 \pm 11.65
Left temporal lobe		Right temporal lobe	
D _{mean}	24.78 \pm 6.82	D _{mean}	23.54 \pm 6.46
D _{max}	73.71 \pm 6.46	D _{max}	72.42 \pm 7.03
Calcarine sulcus		Lingual gyrus	
D _{mean}	7.85 \pm 1.61	D _{mean}	8.81 \pm 1.01
Cuneus		Precuneus	
D _{mean}	6.58 \pm 0.88	D _{mean}	1.41 \pm 0.12
Fusiform gyrus		Cerebellum	
D _{mean}	25.31 \pm 8.53	D _{mean}	27.66 \pm 7.63
Parahippocampus		Hippocampus	
D _{mean}	21.80 \pm 6.05	D _{mean}	28.03 \pm 6.96
Cingulate cortex		Superior occipital gyrus	
D _{mean}	2.71 \pm 2.04	D _{mean}	7.01 \pm 1.69
Superior frontal gyrus		Inferior frontal gyrus	
D _{mean}	2.17 \pm 0.22	D _{mean}	14.70 \pm 2.04
Inferior occipital gyrus		Medial prefrontal gyrus	
D _{mean}	10.24 \pm 1.18	D _{mean}	7.44 \pm 4.39

D_{max}: Maximum dose; D_{mean}: Mean dose; NPC: Nasopharyngeal carcinoma; OARs: Organs at risk; SD: Standard deviation.

RT. However, no significant correlations were found between the functional connections and MoCA tests. This is most likely due to our short intervals after RT (only 1 day), and the longitudinal designs of long-term follow-up are continuously needed. It is worth mentioning that the participants included were from two independent samples, and our self-controlled study may provide more direct evidence about the alterations of the functional network.

It is noteworthy that parahippocampal function also showed a significant reduction in the FC results. Previous studies have suggested that radiation can induce neural microenvironment changes and alterations in the cellular synapses for neurotransmitters such as N-methyl-D-aspartate and gamma-aminobutyric acid after irradiation utilizing *ex vivo* brain slices.^[12,34] Additionally, based on a rodent model, radiation can induce transient hypoxia that may reverse learning and memory abilities.^[35] These biochemical modifications may provide evidence for the basic functional changes. Presently, it has been proven that the parahippocampus is essential for long-term memory processing, especially for spatial memory, learning, and audition.^[36,37] Our findings showed that the abnormality of the parahippocampus may reveal the reasons that NPC patients displayed memory loss and language ability deficits after the completion of RT in 12 to 26 months, whereas no organic temporal lobe abnormality was found

in the images.^[8] More systematic studies about the alterations in NPC patients after RT need to be conducted.

Compared with controls, there were no significant differences in ALFF values and FC before RT. This is not surprising because the tumor is in the nasopharynx, and patients receive no treatment before they are recruited. After treatment, we found that there were some cerebral function regions that presented significant changes, including the lingual gyrus, calcarine sulcus, medial prefrontal gyrus, cingulate cortex, cerebellum, parahippocampal gyrus, hippocampus, fusiform gyrus, inferior frontal gyrus, inferior occipital gyrus, and precuneus. These alteration regions were extensive and unconnected, likely because of irradiation and disease; functional changes could occur following carotid artery blood supply insufficiency from the tumors or metastatic lymph nodes invading the neck and skull base.^[38]

Some limitations of this study should be considered. First, the statistical power of the results is limited. Given the small sample size, the findings in the present study are exploratory, and the results should be considered with caution. Second, although there were no statistically significant results when we compared the ALFF data of patients with and without chemotherapy (seven *vs.* eight) in an independent pilot test, the interference of concurrent

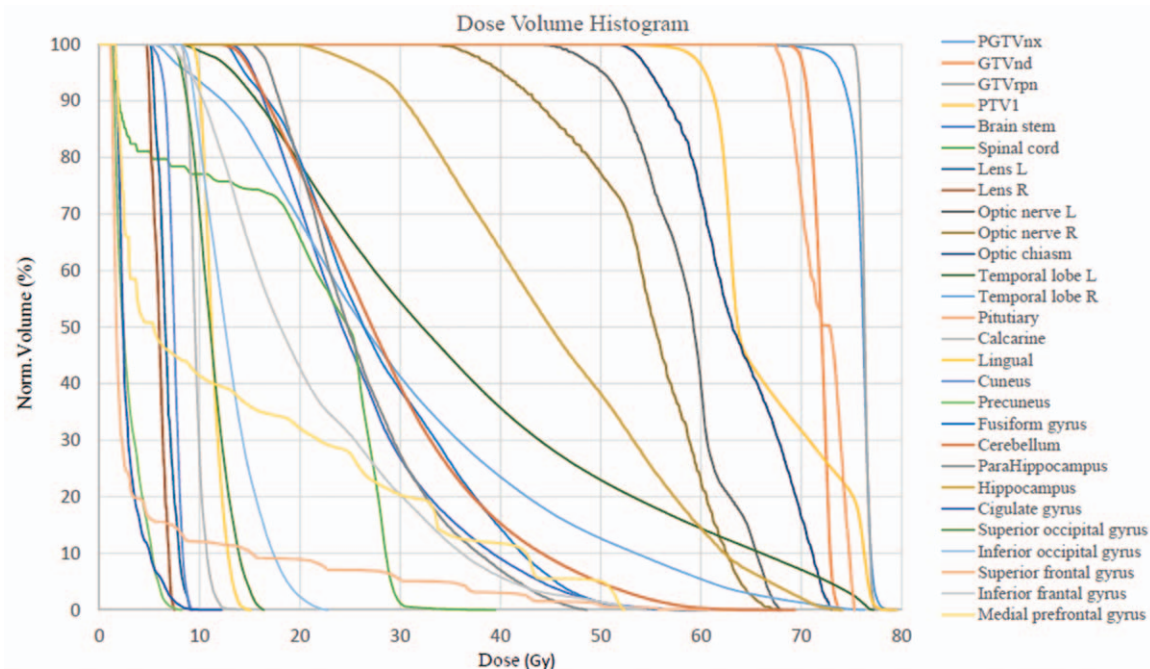


Figure 3: Dose–volume histogram of one representative NPC patient. GTVnd: Gross tumor volume of positive neck lymph nodes; GTVrpn: Gross tumor volume of retropharyngeal lymph nodes; NPC: Nasopharyngeal carcinoma; PGTVnx: Planning gross tumor volume of nasopharynx; PTV1: High risk planning target volume.

chemotherapy should be considered. Future studies need more subgroups to clarify the damage of RT to NPC patients.

In conclusion, the current study revealed that RT in NPC patients leads to regional synchronous neural activity and FC alterations in the short term. These findings provide new insight into the neural system effects of the RT mechanism. The long-term follow-up of patients with NPC may help clarify how alterations in brain function evolve over time and how these changes relate to the treatment sensibility and whether these functional changes could recover. These findings also suggest that novel neuroimaging approaches have the potential to provide useful biomarkers to both investigate the mechanism of RT and tracking clinical dosage effects to optimize and individualize patient treatment.

Funding

This work was supported by grants from the National Natural Science Foundation of China (No. 81402528, No. 11275270)

Conflicts of interest

None.

References

- Chang ET, Adami HO. The enigmatic epidemiology of nasopharyngeal carcinoma. *Cancer Epidemiol Biomarkers Prev* 2006;15:1765–1777. doi: 10.1158/1055-9965.EPI-06-0353.
- Lam LC, Leung SF, Chan YL. Progress of memory function after radiation therapy in patients with nasopharyngeal carcinoma. *J Neuropsychiatry Clin Neurosci* 2003;15:90–97. doi: 10.1176/jnp.15.1.90.
- Wei WI, Sham JS. Nasopharyngeal carcinoma. *Lancet* 2005;365:2041–2054. doi: 10.1016/S0140-6736(05)66698-6.
- Cheung MC, Chan AS, Law SC, Chan JH, Tse VK. Impact of radionecrosis on cognitive dysfunction in patients after radiotherapy for nasopharyngeal carcinoma. *Cancer* 2003;97:2019–2026. doi: 10.1002/cncr.11295.
- Tang Y, Luo D, Rong X, Shi X, Peng Y. Psychological disorders, cognitive dysfunction and quality of life in nasopharyngeal carcinoma patients with radiation-induced brain injury. *PLoS One* 2012;7:e36529. doi: 10.1371/journal.pone.0036529.
- Cheung M, Chan AS, Law SC, Chan JH, Tse VK. Cognitive function of patients with nasopharyngeal carcinoma with and without temporal lobe radionecrosis. *Arch Neurol* 2000;57:1347–1352. doi: 10.1001/archneur.57.9.1347.
- Zheng Y, Han F, Xiao W, Xiang Y, Lu L, Deng X, *et al.* Analysis of late toxicity in nasopharyngeal carcinoma patients treated with intensity modulated radiation therapy. *Radiat Oncol* 2015;10:17. doi: 10.1186/s13014-014-0326-z.
- Hsiao KY, Yeh SA, Chang CC, Tsai PC, Wu JM, Gau JS. Cognitive function before and after intensity-modulated radiation therapy in patients with nasopharyngeal carcinoma: a prospective study. *Int J Radiat Oncol Biol Phys* 2010;77:722–726. doi: 10.1016/j.ijrobp.2009.06.080.
- Tofilon PJ, Fike JR. The radioresponse of the central nervous system: a dynamic process. *Radiat Res* 2000;153:357–370. doi: 10.1667/0033-7587(2000)153[0357:TROTCN]2.0.CO;2.
- Fike JR, Rosi S, Limoli CL. Neural precursor cells and central nervous system radiation sensitivity. *Semin Radiat Oncol* 2009;19:122–132. doi: 10.1016/j.semradonc.2008.12.003.
- Parihar VK, Limoli CL. Cranial irradiation compromises neuronal architecture in the hippocampus. *Proc Natl Acad Sci U S A* 2013;110:12822–12827. doi: 10.1073/pnas.1307301110.
- Wu PH, Coultrap S, Pinnix C, Davies KD, Tailor R, Ang KK, *et al.* Radiation induces acute alterations in neuronal function. *PLoS One* 2012;7:e37677. doi: 10.1371/journal.pone.0037677.
- Monje M, Thomason ME, Rigolo L, Wang Y, Waber DP, Sallan SE, *et al.* Functional and structural differences in the hippocampus associated with memory deficits in adult survivors of acute lymphoblastic leukemia. *Pediatr Blood Cancer* 2013;60:293–300. doi: 10.1002/psc.24263.
- Ma Q, Wu D, Zeng LL, Shen H, Hu D, Qiu S. Radiation-induced functional connectivity alterations in nasopharyngeal carcinoma patients with radiotherapy. *Medicine (Baltimore)* 2016;95:e4275. doi: 10.1097/MD.0000000000004275.

15. Ma Q, Zeng LL, Qin J, Luo Z, Su J, Wu D, *et al.* Radiation-induced cerebellar-cerebral functional connectivity alterations in nasopharyngeal carcinoma patients. *Neuroreport* 2017;28:705–711. doi: 10.1097/WNR.0000000000000813.
16. Damoiseaux JS, Rombouts SA, Barkhof F, Scheltens P, Stam CJ, Smith SM, *et al.* Consistent resting-state networks across healthy subjects. *Proc Natl Acad Sci U S A* 2006;103:13848–13853. doi: 10.1073/pnas.0601417103.
17. Goncalves SI, de Munck JC, Pouwels PJ, Schoonhoven R, Kuijter JP, Maurits NM, *et al.* Correlating the alpha rhythm to BOLD using simultaneous EEG/fMRI: inter-subject variability. *Neuroimage* 2006;30:203–213. doi: 10.1016/j.neuroimage.2005.09.062.
18. Han Y, Wang J, Zhao Z, Min B, Lu J, Li K, *et al.* Frequency-dependent changes in the amplitude of low-frequency fluctuations in amnesic mild cognitive impairment: a resting-state fMRI study. *Neuroimage* 2011;55:287–295. doi: 10.1016/j.neuroimage.2010.11.059.
19. Liu CH, Li F, Li SF, Wang YJ, Tie CL, Wu HY, *et al.* Abnormal baseline brain activity in bipolar depression: a resting state functional magnetic resonance imaging study. *Psychiatry Res* 2012;203:175–179. doi: 10.1016/j.psychres.2012.02.007.
20. Biswal B, Yetkin FZ, Haughton VM, Hyde JS. Functional connectivity in the motor cortex of resting human brain using echo-planar MRI. *Magn Reson Med* 1995;34:537–541. doi: 10.1002/mrm.1910340409.
21. Kublbock M, Woletz M, Hoflich A, Sladky R, Kranz GS, Hoffmann A, *et al.* Stability of low-frequency fluctuation amplitudes in prolonged resting-state fMRI. *Neuroimage* 2014;103:249–257. doi: 10.1016/j.neuroimage.2014.09.038.
22. Chao-Gan Y, Yu-Feng Z. DPARSF: a MATLAB toolbox for “Pipeline” data analysis of resting-state fMRI. *Front Syst Neurosci* 2010;4:13. doi: 10.3389/fnsys.2010.00013.
23. Lui S, Li T, Deng W, Jiang L, Wu Q, Tang H, *et al.* Short-term effects of antipsychotic treatment on cerebral function in drug-naive first-episode schizophrenia revealed by “resting state” functional magnetic resonance imaging. *Arch Gen Psychiatry* 2010;67:783–792. doi: 10.1001/archgenpsychiatry.2010.84.
24. Song XW, Dong ZY, Long XY, Li SF, Zuo XN, Zhu CZ, *et al.* REST: a toolkit for resting-state functional magnetic resonance imaging data processing. *PLoS One* 2011;6:e25031. doi: 10.1371/journal.pone.0025031.
25. Anurova I, Renier LA, De Volder AG, Carlson S, Rauschecker JP. Relationship between cortical thickness and functional activation in the early blind. *Cereb Cortex* 2015;25:2035–2048. doi: 10.1093/cercor/bhu009.
26. Beason-Held LL, Purpura KP, Krasuski JS, Maisog JM, Daly EM, Mangot DJ, *et al.* Cortical regions involved in visual texture perception: a fMRI study. *Brain Res Cogn Brain Res* 1998;7:111–118. doi: 10.1016/S0926-6410(98)00015-9.
27. Zhao Z, Lan Y, Bai S, Shen J, Xiao S, Lv R, *et al.* Late-onset radiation-induced optic neuropathy after radiotherapy for nasopharyngeal carcinoma. *J Clin Neurosci* 2013;20:702–706. doi: 10.1016/j.jocn.2012.05.034.
28. Golby A, Silverberg G, Race E, Gabrieli S, O’Shea J, Knierim K, *et al.* Memory encoding in Alzheimer’s disease: an fMRI study of explicit and implicit memory. *Brain* 2005;128:773–787. doi: 10.1093/brain/awh400.
29. Moon CM, Jeong GW. Functional and morphological alterations associated with working memory dysfunction in patients with generalized anxiety disorder. *Acta Radiol* 2017;58:344–352. doi: 10.1177/0284185116649794.
30. Raichle ME, MacLeod AM, Snyder AZ, Powers WJ, Gusnard DA, Shulman GL. A default mode of brain function. *Proc Natl Acad Sci U S A* 2001;98:676–682. doi: 10.1073/pnas.98.2.676.
31. Greicius MD, Krasnow B, Reiss AL, Menon V. Functional connectivity in the resting brain: a network analysis of the default mode hypothesis. *Proc Natl Acad Sci U S A* 2003;100:253–258. doi: 10.1073/pnas.0135058100.
32. Damoiseaux JS, Beckmann CF, Arigita EJ, Barkhof F, Scheltens P, Stam CJ, *et al.* Reduced resting-state brain activity in the “default network” in normal aging. *Cereb Cortex* 2008;18:1856–1864. doi: 10.1093/cercor/bhm207.
33. Greicius MD, Srivastava G, Reiss AL, Menon V. Default-mode network activity distinguishes Alzheimer’s disease from healthy aging: evidence from functional MRI. *Proc Natl Acad Sci U S A* 2004;101:4637–4642. doi: 10.1073/pnas.0308627101.
34. Monje ML, Mizumatsu S, Fike JR, Palmer TD. Irradiation induces neural precursor-cell dysfunction. *Nat Med* 2002;8:955–962. doi: 10.1038/nm749.
35. Warrington JP, Csiszar A, Mitschelen M, Lee YW, Sonntag WE. Whole brain radiation-induced impairments in learning and memory are time-sensitive and reversible by systemic hypoxia. *PLoS One* 2012;7:e30444. doi: 10.1371/journal.pone.0030444.
36. Lech RK, Suchan B. The medial temporal lobe: memory and beyond. *Behav Brain Res* 2013;254:45–49. doi: 10.1016/j.bbr.2013.06.009.
37. Jeneson A, Squire LR. Working memory, long-term memory, and medial temporal lobe function. *Learn Mem* 2012;19:15–25. doi: 10.1101/lm.024018.111.
38. Abayomi OK. Pathogenesis of irradiation-induced cognitive dysfunction. *Acta Oncol* 1996;35:659–663. doi: 10.3109/02841869609083995.

How to cite this article: Ren WT, Li YX, Wang K, Gao L, Yi JL, Huang XD, Luo JW, Wu RY, Yang Y, Wang JY, Wang WQ, Wang JB, Ye F, Ouyang H, Dai JR. Cerebral functional abnormalities in patients with nasopharyngeal carcinoma after radiotherapy: an observational magnetic resonance resting-state study. *Chin Med J* 2019;132:1563–1571. doi: 10.1097/CM9.0000000000000277